

To appear in A. J., February 1998

The He II Opacity of the Lyman α Forest and the Intergalactic Medium

Wei Zheng, Arthur F. Davidsen, and Gerard A. Kriss

Center for Astrophysical Sciences

Johns Hopkins University, Baltimore, MD 21218

zheng@pha.jhu.edu afd@pha.jhu.edu gak@pha.jhu.edu

ABSTRACT

Primordial baryonic matter in the vast intergalactic space may be traced with Ly α resonance absorption by neutral hydrogen and singly ionized helium. The wavelength-averaged He II opacity shortward of $304(1+z)$ Å, as measured by low-resolution UV spectroscopy, is at least 4.5 times the H I opacity shortward of $1216(1+z)$ Å. While a part of the He II opacity arises from the intergalactic regions that produce the known Ly α forest, it has been argued whether the He II opacity may be *entirely* attributable to these observed lines. Based on the empirical formulas governing the distribution of Ly α forest absorption, we use a Monte-Carlo technique to calculate the average He II optical depth produced by these forest lines.

The He II counterparts of the Ly α forest lines are highly saturated, and hence their contributions to the observed opacity is limited. Assuming a He⁺/H₀ population ratio of 100 and that the power-law distribution $dn/dN \propto N^{-1.5}$ can be extended to a neutral hydrogen column density of $N_{HI} = 2 \times 10^{12}$ cm⁻², the contribution from these forest lines may account for a He II opacity that is $\lesssim 3$ times the H I opacity. Our simulated He II spectrum of the quasar Q0302-003, based on the fitted lines in the high-resolution Keck spectrum, yields a forest optical depth of ~ 0.9 , less than half of the observed He II opacity. Therefore, a substantial contribution to He II absorption arises from extremely tenuous regions of intergalactic gas that are beyond the observational limits for H I absorption. He II spectra at higher resolution are a sensitive tool to explore the properties of these small-scale fluctuations that fill $\sim 80\%$ of the intergalactic space and contain a significant part of the baryonic matter in the early universe.

Subject headings: intergalactic medium; quasars –: absorption lines; cosmology

1. INTRODUCTION

Shortly after the discovery of quasars, it was found that the flux shortward of the redshifted Ly α emission at $(1+z) 1216 \text{ \AA}$ is depressed. Gunn & Peterson (1965) suggested that this may be due to the accumulated Ly α absorption by a uniform, diffuse intergalactic medium (IGM) at high redshifts. Optical spectroscopy at improved spectral resolution (Lynds 1971; Sargent et al. 1980) found that the absorption arises from numerous narrow features referred to as “the Ly α forest”. The lack of a smooth depression in flux (the Gunn-Peterson effect, see Steidel & Sargent 1987 and references therein) has led to the conclusion that the IGM is highly ionized by a metagalactic UV radiation field in the early universe (Fields 1972; Bechtold et al. 1987; Miralda-Escudé & Ostriker 1990). Premordial intergalactic helium should also produce absorption features, notably He II Ly α . Recent theoretical models of the IGM evolution (Cen et al. 1994; Zhang, Anninos, & Norman 1995; Miralda-Escudé et al. 1996; Hernquist et al. 1996; Bi & Davidsen 1997) suggest that there is no distinct boundary between a diffuse component of the IGM and discrete forest clouds. The evolution of the universe leads to density fluctuations on all scales. Evolving structures produce absorption features with a column-density distribution similar to that observed in the Ly α forest. The features of the lowest column density arise in underdense portions of the IGM and contribute most to the He II opacity. In conventional terms, forest lines are referred to as those that can be identified with optical spectroscopy. Most of them have column densities of 10^{13} cm^{-2} or higher, and the Keck HIRES spectra have identified absorption features as weak as $N = 2 \times 10^{12} \text{ cm}^{-2}$ (Hu et al. 1995).

If the UV background radiation is derived mainly from quasar radiation, its EUV photons are able to ionize He $^+$, and hence the intergalactic helium is likely to be primarily in the form of He $^{++}$ (Madau 1992). However, because of the high ionization level for He $^+$, the He $^+$ population in the IGM would be significantly higher than that of H $_0$ (Sargent et al. 1980; Miralda-Escudé & Ostriker 1990) and may hence be more easily detected. He II Ly α absorption is within the spectroscopic capability of the Hubble Space Telescope (*HST*) for quasars with $z > 3$ and of the Hopkins Ultraviolet Telescope (HUT) for quasars of $z > 2$.

Jakobsen et al. (1994) reported a cutoff in flux shortward of redshifted He II Ly α emission in the *HST* Faint Object Camera (FOC) prism spectrum of the quasar Q0302-003 ($z_{\text{em}} = 3.286$), with optical depth $\tau > 1.7$ at 90% confidence level. Follow-up *HST HRS* observations (Hogan, Anderson & Rugers 1997) find that the average He II optical depth $\tau_{\text{HeII}} = 2.0_{-0.5}^{+1.0}$ (95% confidence level) at redshift $z \approx 3.15$. The spectrum of the quasar HS1700+64 ($z_{\text{em}} = 2.743$) obtained with HUT had previously provided a measurement of the average optical depth $\tau = 1.00 \pm 0.07$ at $z \approx 2.4$ (Davidsen, Kriss, & Zheng 1996). The long-sought He II absorption confirms primordial intergalactic helium as predicted by the Big Bang theory and provides insights into the ionization state and density of the IGM.

Neither of these observations, however, can resolve He II Ly α forest lines, hence the observed opacity in the spectral region shortward of $304(1+z) \text{ \AA}$ is a blend of absorption features arising

from regions of various density. The regions with very small-scale fluctuations in the IGM produce absorption features that are below the observational limit, i.e. they have with the neutral hydrogen column density $N_{HI} < 2 \times 10^{12} \text{ cm}^{-2}$ (N hereafter). By precisely modeling the expected contribution of the observed He II Ly α forest features based on measurements of the H I Ly α forest, one can hope to disentangle the contributions of the different regions of the IGM above and below the threshold column density $N = 2 \times 10^{12} \text{ cm}^{-2}$.

Several techniques have been used to estimate the likely contribution of the observed forest lines to the He II opacity. Jakobsen et al. (1994), Madau & Meiksin (1994), and Giroux, Fardal, & Shull (1995) all used the formula

$$\tau(z) = \frac{dn}{dz} \frac{\langle W_\lambda \rangle}{\lambda} (1+z) \quad (1)$$

where dn/dz is the number of lines per unit redshift and $\langle W_\lambda \rangle$ is the mean rest-frame equivalent width of He II Ly α lines averaged over the assumed distribution in column density (Møller & Jakobsen 1990). This in turn is based on the optical depth for a random distribution of absorbing clouds as described by Paresce, McKee, & Bowyer (1980). Jakobsen et al. (1994) concluded that the He II forest may not account for the observed He II opacity in their spectrum of Q0302-003 unless there is a significant population of clouds with $N < 10^{13} \text{ cm}^{-2}$. Madau & Meiksin (1994) and Giroux et al. (1995) explored further how the forest opacity is influenced by the helium to hydrogen velocity-dispersion ratio ($\xi = b_{He}/b_H$). Starting from a relatively high estimate of the H I opacity in the Ly α forest toward Q0302-003, they found that all the observed opacity can be attributed to forest lines with $N > 10^{12} \text{ cm}^{-2}$. A key assumption in the method upon which all these studies are based, however, is that the absorption at any wavelength is due to only a single cloud. When the minimum column density is extended much below 10^{13} cm^{-2} , observed lines begin to overlap significantly, and this approximation breaks down.

Songaila, Hu, & Cowie (1995) used two different approaches. The first directly used their high resolution, high S/N ratio spectrum of the Ly α forest in Q0302-003. For a normalized spectrum of the H I forest with intensity given by $S(4\lambda)$, the normalized spectrum of the He II forest is given by $S(\lambda) = [S(4\lambda)]^{\frac{\eta}{4}}$, where η is the population ratio of He⁺ to H₀. The principle drawback of this elegant and rather straightforward method is that it is extremely sensitive to the S/N level and to the fitted continuum level. Even at S/N = 50, noise in the data is amplified into features in the He II forest with optical depth ~ 0.4 if $\eta = 80$. With this approach, metal-line systems in the H I forest are also incorrectly incorporated into the predicted He II opacity.

Their second approach used the formula developed by Miralda-Escudé (1993) to describe the relative opacities in the H I and He II forest:

$$\tau_{\text{HeII}} = \tau_{\text{HI}} \left(\frac{\eta}{4}\right)^{\beta-1} \xi^{2-\beta}, \quad (2)$$

where β is the power law index of the Ly α forest column density distribution. This formula is only valid, however, if the distribution includes lines that are optically thin for He II as well as H I.

As we will show below, this assumption holds only if the power law distribution of the H I forest column densities extends to $N \ll 10^{12} \text{ cm}^{-2}$.

Previous work either claim that it cannot be determined whether the observed He II opacity is due to the known forest lines (Jakobsen 1996), or it can entirely be attributed to them (Songaila et al. 1995). In this paper we present improved calculations of the line opacity produced by the He II Ly α forest. To overcome the limitations of previous work, we use a Monte-Carlo technique to simulate the absorption spectrum of He II forest. While the forest-line interpretation may not describe the physical nature of the IGM, we use it to compare with the published results. Under this scenario, we explore how variations in the minimum column density, in the He⁺ to H₀ population ratio (η) and in the ratio of helium to hydrogen velocity dispersion (ξ) affect the contribution of the known forest components to the total He II opacity. Our calculations yield He II opacities smaller than previously estimated, and we conclude that forest lines with $N > 2 \times 10^{12} \text{ cm}^{-2}$ *cannot* account for the observed He II opacity with the parameters commonly assumed.

2. OPACITY CALCULATIONS

To evaluate the opacity in single lines we use the standard curve-of-growth method with a Voigt profile (see Press & Rybicki 1993). Although deviations from Voigt profiles are expected in recent models due to the spatial extension of the IGM fluctuation, the effect is not significant for most lines. A typical physical size of such a structure is about $0.14h^{-1} \text{ Mpc}$ (Bi & Davidsen 1997), equivalent to 14 km s^{-1} in the velocity space. This is smaller than the characteristic velocity of $\sim 30 \text{ km s}^{-1}$ (Press & Rybicki 1993). The contributions from density wings at $\sim 100 \text{ km s}^{-1}$ may become noticeable only for lines with $N > 10^{14} \text{ cm}^{-2}$. Line blending due to thermal and/or turbulence velocity affect all models, and therefore Voigt profiles are a fair match at the first order.

The most important factor governing the He II opacity is η . For very tenuous gas ($N(\text{HeII}) \ll 10^{14} \text{ cm}^{-2}$), the He II absorption decrement is proportional to the optical opacity, but it is not the case for most forest lines, due to saturation effects. For Ly α lines of equivalent width $W > 0.3 \text{ \AA}$, the He II to H I opacity ratio for a single feature changes very slowly with η as both He II and H I lines are saturated and their equivalent widths depend only weakly on the column density.

The H I and He II curves are similar, as He⁺ ions are hydrogenic. The Doppler parameter for helium depends on ξ , which lies between 0.5 and 1.0, depending on the nature of the line broadening. Observations by Cowie et al. (1995) suggest $\xi \sim 0.8$. We will use this value in most of our calculations as the results can be scaled to suit other ξ values.

Assuming $\xi = 0.8$, we show in Fig. 1 the He II to H I decrement ratio of a single absorption feature as a function of column density for three values of the Doppler parameter b_H : 20, 30, and 50 km s^{-1} . For a typical value of $b_H = 30 \text{ km s}^{-1}$, this ratio is near unity for $N \approx 10^{14-15} \text{ cm}^{-2}$. At higher densities, it increases as the damping wings contribute appreciably to the He II Ly α

absorption. At lower densities, the ratio becomes high as the H I absorption lies on the linear part of the curve and decreases. From Fig. 1 we can immediately infer that the opacity of the He II forest will depend strongly on the minimum column density chosen for the Ly α forest.

To calculate the wavelength-averaged opacity of the He II Ly α forest, we start with the standard empirical description of the H I Ly α forest population. The number of Ly α forest absorption features, n , in quasar spectra may be described by

$$\frac{\partial^2 n}{\partial z \partial N} = A(1+z)^\gamma N^{-\beta} \quad (3)$$

(Peterson 1978; Tytler 1987; Press & Rybicki 1993). We adopt $\beta = 1.5$ and $\gamma = 2.4$ from Miralda-Escudé & Ostriker (1990). The normalization factor A affects the forest opacity appreciably, and it can vary depending on the particular line of sight. We choose A to be consistent with the number of lines and the measured H I forest opacity for the particular quasar under study. The Doppler parameter b is assumed to follow a Γ -function distribution:

$$p(b) db \propto b^{(b_0/b^*)-1} \exp(-b/b^*) db, \quad (4)$$

where $b_0 = 38 \text{ km s}^{-1}$ and $b^* = 14 \text{ km s}^{-1}$ (Press & Rybicki 1993).

Our Monte-Carlo method randomly generates centroid wavelengths, column densities and Doppler parameters for each line in the H I forest according to Eq. 3 (for a given minimum column density) and the Doppler-parameter distribution of Eq. 4. The Voigt profiles of the selected lines are then calculated in the quasar rest frame with a spacing of 0.01 \AA ($\sim 3 \text{ km s}^{-1}$). The product of these profiles gives the total transmission of the H I forest. The effect of line blending is naturally taken into consideration in this treatment. Given the transmission of the H I forest we calculate the decrement D_{HI} and express the wavelength-averaged forest optical depth as $\tau_{\text{HI}} = -\ln(1 - D_{\text{HI}})$. Individual realizations of the forest opacity in this method show fluctuations of $\sim 15\%$ due to the random line blending. For each set of parameters we run 10 simulations and average the results to obtain the final opacity values.

The corresponding He II forest is constructed by changing the column density of each simulated line from N to ηN , and the Doppler parameter from b to ξb . The average decrement for He II, D_{HeII} , is calculated, and the wavelength-averaged optical depth is given again by $\tau_{\text{HeII}} = -\ln(1 - D_{\text{HeII}})$.

To illustrate our results, we present calculations for a quasar redshift $z_{\text{em}} = 2.74$ for comparison to the HUT observations of HS1700+64 (Davidsen et al. 1996). We normalize the column-density distribution using $A = 2.0 \times 10^7$ to match the line number density measured for this quasar by Rodríguez-Pascual et al. (1995) and Zheng et al. (1997). We use the 1050–1170 \AA wavelength range (in the rest frame) to calculate the H I opacity and rest-frame wavelengths 262–292 \AA for the He II opacity. These wavelength ranges, free of confusion from the proximity effect and Ly β lines, has often been used to calculate the average absorption decrement D_A (Jenkins & Ostriker 1991; Press, Rybicki, & Schneider 1993). Fig. 2 displays the average He II forest optical depth as a function of the minimum column density for two values of redshift. The effect of changing η is

shown by several curves in the upper panels of the figure. The lower panels show the sensitivity of the results to the assumed value of ξ with η held fixed at 100.

The behavior of the He II forest opacity shown in Fig. 2 can be qualitatively understood in terms of the He II to H I decrement ratios illustrated in Fig. 1. The total H I opacity increases as the minimum column density is lowered, but it levels out at $N \approx 10^{13} \text{ cm}^{-2}$. This is because at low column densities H I absorption is proportional to the column density and becomes insignificant as lines move off the saturated portion of the curve of growth. The He II opacity, on the other hand, continues to increase significantly as the minimum column density is lowered toward $N \approx 10^{11} \text{ cm}^{-2}$. This is because He II absorption is still in the flat part of the curve of growth. The opacity ratio ρ therefore becomes higher when more weak forest lines are included. Note that strong lines ($N > 2 \times 10^{13} \text{ cm}^{-2}$) produce nearly the same amount of absorption for He II and H I, but they contribute only $\sim 30\%$ of the total He II opacity for $\eta = 100$. Weak lines ($2 \times 10^{12} \text{ cm}^{-2} < N < 2 \times 10^{13} \text{ cm}^{-2}$) contribute $\sim 40\%$ of the total He II opacity, compared with only $\sim 5\%$ for H I.

We expect the forest opacity to increase with redshift in proportion to the number of H I forest clouds within the wavelength interval of interest. Since $\Delta N \propto (1+z)^\gamma \Delta z$, and $\Delta z = (1+z)\Delta\lambda_o$, where $\Delta\lambda_o$ is the rest frame wavelength interval, the He II forest opacity should have a redshift-dependence of $(1+z)^{1+\gamma}$. To verify this we have also made calculations applicable to the quasar Q0302-003. To match the wavelength range used by Hogan et al. (1997) to measure the He II opacity in their GHRS spectrum, we use the rest-frame wavelength ranges of 1157-1195 Å and 289-299 Å for the H I and He II forest, respectively. We normalize the column density distribution to give a total H I forest opacity of 0.21 (see below). These results are shown in Fig. 2b.

Given opacities for both the He II and H I Ly α forest, we can calculate the ratio of their average opacities, ρ , as a function of the minimum column density. This ratio is shown in Fig. 3 for $z_{em} = 2.74$. (A comparison to ρ calculated for $z_{em} = 3.3$ indicates that the behavior of ρ is virtually independent of redshift over this range.) Qualitatively this is to be expected, following the derivation of ρ in the optically thin limit in Eq. 3. However, this relation assumes that the decrement produced by an absorption line is proportional to its central optical depth. This is only correct for optically thin lines (i.e., a centroid optical depth not significantly greater than unity) and hence may not be applied to strong forest lines, which account for $\sim 60\%$ of the H I optical opacity. At column densities $N \approx 10^{14} \text{ cm}^{-2}$, for example, the value of ρ is nearly unity even for $\eta \gg 1$. As shown in Fig. 3, only at column densities $N \ll 10^{12} \text{ cm}^{-2}$ does ρ approach the value predicted by Eq. 2 (assuming a reasonably high value of $\eta > 50$). Fig. 3 also shows that applying Eq. 2 at $N_{min} \approx 2 \times 10^{12} \text{ cm}^{-2}$ leads to a considerable overestimation of the He II forest opacity.

3. COMPARISON TO PREVIOUS WORK

For comparison to previous work on the quasar Q0302-003, we refer to the He II opacities shown in Fig. 2*b*. For parameters typical of those used by Jakobsen et al. (1994), Madau & Meiksin (1994) and Giroux et al. (1995), i.e. $\eta = 100$, $b_H = 30 \text{ km s}^{-1}$, $\xi = 0.5$, and $N > 10^{12} \text{ cm}^{-2}$, we obtain an optical depth for the He II forest $\tau_{\text{HeII}} \approx 0.53$. Their calculated opacities are, approximately, 0.9, 1.3 and 1.1, respectively. These values are larger than ours by $\sim 70 - 150\%$. A difference at a level of $\sim 15\%$ is due to line blending. Weak lines, when blended with strong ones, do not decrease the transmission appreciably in already blank regions of the spectrum. We estimate that, at $z \approx 3$, $\sim 15\%$ of the spectral region is virtually blank due to the high opacity of strong lines, implying that at least $\sim 15\%$ of the He II opacity from weak lines would not be realized. The rest of the discrepancy may be attributed to the normalization chosen for the distribution of H I Ly α forest lines (Eq. 3). A high normalization leads to a high H I opacity as well as a high He II opacity. The average H I optical depth in the spectrum of quasar Q0302-003 is particularly low, with $\tau_{\text{HI}} \approx 0.21$ between 5000 and 5200 Å as estimated from Fig. 1 of Songaila et al. (1995). This is mainly due to a void in this quasar spectrum (Dobrzycki & Bechtold 1991; Nath & Sethi 1996). For comparison, the H I forest opacities for the line distributions used by Jakobsen et al. (1994), Madau & Meiksin (1994) and Giroux et al. (1995) are 0.35, 0.55 and 0.44, respectively.

An even larger discrepancy exists between our result and that of Songaila et al. (1995) who simulated a He II spectrum based on their Keck spectrum of the quasar Q0302-003. Their simulated He II spectrum based on the assumed values of $\eta = 80$ and $\xi = 1.0$ produces a very high value of $\tau_{\text{HeII}} \approx 1.6$, corresponding to $\rho \approx 5$. As we showed in §2, however, saturation in the He II Ly α lines prevents ρ from reaching values this high unless the minimum column density is significantly lower than 10^{12} cm^{-2} . Our simulations using the same parameters yield $\tau_{\text{HeII}} \approx 0.9$, i.e. $\rho \approx 3$.

The large difference between our result and that of Songaila et al. (1995), on the order of $\Delta\tau_{\text{HeII}} \approx 0.7$, probably arises from several factors: (1) noise can contribute significantly to the He II opacity in their simulated spectrum. $\eta = 80$ represents an optical depth ratio of 20. At a noise level of 2% (S/N = 50 per resolution element), an amplification by 20 may produce an erroneous optical depth of ~ 0.4 . (2) Even at an infinite S/N level, the He II spectrum simulated by Songaila et al. (1995) contains not only the contribution from lines with $N > 2 \times 10^{12} \text{ cm}^{-2}$, but also those below this threshold that have not been identified. Some very broad but shallow lines have been seen in the Ly α forest (Kirkman & Tytler 1995), and they may be from clouds with $N < 2 \times 10^{12} \text{ cm}^{-2}$. (3) Metal lines are treated as additional forest lines. Observations have shown that metal lines often account for more than 5% of the total absorption lines in the Ly α forest (Carswell et al. 1991; Rauch et al. 1993). In some quasars such as HS1700+64 (Rodríguez-Pascual et al. 1995) the density of metal lines in the Ly α forest region is about 20% of the true Ly α forest lines. When “amplifying” the whole H I forest spectrum these metal lines may add a significant amount of erroneous opacity to the simulated He II spectrum.

To avoid these problems we constructed a He II spectrum using the fitted Ly α forest lines in

Q0302-003 tabulated by Hu et al. (1995) instead of the real spectrum. In the optical range of 4400–5000 Å, Hu et al. (1995) identified 258 forest lines with $N \geq 2 \times 10^{12} \text{ cm}^{-2}$. Using their b and N values we construct an H I spectrum and another for He II, assuming $\eta = 80$ and $\xi = 1.0$. Because the reconstructed spectrum contains neither noise, nor weak features of $N < 10^{12} \text{ cm}^{-2}$, nor metal lines, it is different from the real spectrum in some aspects. For example, $\sim 60\%$ of the data points in our reconstructed H I spectrum have optical depths larger than 0.05, in comparison with 75% in the real spectrum (Songaila et al. 1995). From our simulated spectrum we calculate the average He II optical depth in the D_A region to be ~ 0.91 . This value is significantly smaller than that derived by Songaila et al. from the *same* spectrum, but in good agreement with the predictions of our Monte-Carlo technique. Our simulated spectrum is plotted in Fig. 4 and can be compared with Fig. 1 of Songaila et al. (1995).

4. DISCUSSION

Until recently, most studies of the H I Ly α forest were limited to features with column densities exceeding $\sim 10^{13} \text{ cm}^{-2}$. Fig. 2a shows that, for this limiting column, the He II forest can contribute no more than 50% of the total observed opacity even for $\xi = 1.0$ and η as high as 1000. Observations of H I Ly α features with an order of magnitude lower column density in other quasars with the Keck 10-m telescope (Songaila et al. 1995; Hu et al. 1995) suggest that the power-law distribution of the H I Ly α forest may extend to column densities as low as $2 \times 10^{12} \text{ cm}^{-2}$. Even at this limiting column, however, matching the He II opacity observed with HUT requires $\eta > 1000$. The quasar Q0302-003 has been observed with Keck to a limiting column density of $2 \times 10^{12} \text{ cm}^{-2}$. Fig. 2b shows that at this limiting column density $\eta \gg 1000$ is also required to match the observed He II opacity $\tau_{HeII} \approx 2.0$ (Hogan et al. 1997).

Is it possible that the metagalactic background radiation is so soft that $\eta > 1000$? We think it is unlikely. Theoretical calculations of the UV-background radiation produced by the observed quasar population, taking into account filtering by the Ly α forest, predict that η should lie in the range 30 to 100 (Miralda-Escudé & Ostriker 1990; Madau & Meiksin 1994; Haardt & Madau 1996). A mean quasar spectrum (Zheng et al. 1997a) suggest a continuum shape of $f_\nu \approx \nu^{-1.8}$ between 1 and 4 Rydberg, and, if the ionizing field is dominated by quasar radiation, this would lead to $\eta \simeq 100$ (Madau, private communication). Background radiation dominated at low energies by a large contribution from young galaxies could produce $\eta > 1000$ (Miralda-Escudé & Ostriker 1990). Several observational details argue against η being this high, however. First, very soft background radiation would produce a significant proximity profile (Zheng & Davidsen 1995), which is not observed. Second, if the observed He II opacity is derived entirely from forest lines with $N > 2 \times 10^{12} \text{ cm}^{-2}$, there should be spectral windows in which the He II opacity is much lower. In these windows (“voids”) there are no or very few forest lines detected in the Keck spectra of Q0302-003. The recent observations with improved resolution (Hogan et al. 1997) show a

substantial He II opacity even in the spectral voids. The lack of emission peaks corresponding to these voids in the wavelengths shortward of the redshifted He II Ly α emission suggests that the contribution to the total opacity from observed forest lines is limited. Third, the inferred shape of the background ionizing spectrum based on observations of metal lines in Ly α clouds suggests that $\eta < 155$ (Songaila et al. 1995).

If the background radiation is hard enough to ensure $\eta \sim 100$, then the additional opacity required to explain the observations of HS1700+64 and Q0302-003 must arise from a more tenuous part of the IGM. If the minimum column density can be extended to arbitrarily low values so that the formula of Miralda-Escudé (1994) applies, then the HUT observations of $\tau_{\text{HeII}} = 1.00 \pm 0.07$ in HS1700+64 and the H I opacity of 0.22 (Davidsen et al. 1996) imply $\rho = 4.5 \pm 0.5$. For $\xi = 0.8$, the He II to H I population ratio must be $\eta = 100^{+25}_{-20}$. Similarly, for the quasar Q0302-003, we have $\tau_{\text{HeII}} \approx 2.0$ and $\tau_{\text{HI}} = 0.21$ imply $\rho \gtrsim 10$ and $\eta > 180$. Hogan et al. (1997) find that the He II optical depth in the spectral voids of Q0302-003 is ~ 1.3 . In § 3 we estimate the He II opacity produced by the forest lines (Hu et al. 1995) $\tau_{\text{HeII}} \sim 0.9$. The sum of these two terms (2.2) is very close to the measured total He II opacity (2.0), suggesting that our estimate of the forest opacity is quite accurate.

Croft et al. (1997) use gravitation-instability calculations to simulate the He II absorption observed by HUT. Their results confirm that much of the opacity arises in underdense regions in which the H I opacity is very low. It is true that the extension of Eq. 3 to column densities far below 10^{12} cm^{-2} will indeed make forest-line model indistinguishable from the gas-dynamics model. However, the Keck spectrum of HS1700+64 (Zheng et al. 1997b) suggests that, at $z \sim 2.4$, the number of lines with $N < 10^{13} \text{ cm}^{-2}$ is considerably smaller than the extrapolation of a power law predicts. This trend is qualitatively consistent with the cold-dark-matter models (Miralda-Escudé et al. 1996; Bi & Davidsen 1997) that the distribution of forest lines flattens at lower column densities.

5. SUMMARY

Previous work overestimated the contribution from known forest lines. Assuming a column-density distribution for the H I forest with a power-law index $\beta = 1.5$, a He⁺ to H₀ population ratio $\eta = 100$ and velocity dispersion ratio $\xi = 0.8$, we calculate a He II opacity produced by the observed forest lines that is $\sim 3\times$ the H I opacity. This can account for about half of the observed He II opacity along the sight line to the quasars HS1700+64. For Q0302-003, the lower limit to the He II opacity set by the observation is at least $8\times$ the H I opacity, making it more difficult to explain in terms of forest lines. Our results show that about 50% of the He II opacity at $z \sim 3$ is produced by the most tenuous part of the IGM with column density $N < 10^{12} \text{ cm}^{-2}$.

The detection of He II absorption concludes a long pursuit and opens a new window to the

early universe. Because $\tau(\text{HeII})/\tau(\text{HI}) = \eta/4$ and $\eta \gg 1$, He II absorption spectra are sensitive to the underdense region where the early seeds of density fluctuations develop. With future far-UV spectroscopy at higher resolution and sensitivity, we will be able to resolve individual structures along the full paths to the early universe, measure the ionization state, the density, and distribution of baryonic matter in intergalactic space.

This work has been supported by NASA contract NAS-5-27000 to the Johns Hopkins University and grant AR-05821.01-94A from the Space Telescope Science Institute, which is operated by the Association of Universities for Research in Astronomy, Inc., under NASA contract NAS5-26555.

REFERENCES

- Bechtold, J., Weymann, R. J., Lin, Z., & Malkan, M. A. 1987, *ApJ*, 315, 180
- Bi, H., & Davidsen, A. F. 1997, *ApJ*, 479, 523
- Carswell, R. F., Lanzetta, K. M., Parnell, H. C., & Webb, J. K. 1991, *ApJ*, 371, 36
- Cen, R., Miralda-Escudé, J., Ostriker, J. P., & Rauch, M. 1994, *ApJ*, 437, L9
- Cowie, L. L., Songaila, A., Kim, T.-S., & Hu, E. M. 1995, *AJ*, 109, 1522
- Croft, R. A. C., Weinberg, D. H., Katz, N., & Hernquist, L. 1997, *ApJ*, 488, 532
- Davidsen, A. F., Kriss, G. A., & Zheng, W. 1996, *Nature*, 380, 47
- Dobrzycki, A. & Bechtold, J. 1991, *ApJ*, 377, L69
- Field, G. B. 1972, *ARAA*, 10, 227
- Giroux, M. L., Fardal, A. A., & Shull, J. M. 1995, *ApJ*, 451, 477
- Gunn, J. E., & Peterson, B. A. 1965, *ApJ*, 142, 1633
- Haardt, F., & Madau, P. 1996, *ApJ*, 461, 20
- Hernquist, L., Katz, N., Weinberg, D. H., & Miralda-Escudé, J. 1996, *ApJ*, 457, L51
- Hogan, C. J., Anderson, S. F., & Rugers, M. H. 1997, *AJ*, 113, 1495
- Hu, E. M., Kim, T.-S., Cowie, L. L., Songaila, A., & Rauch, M. 1995, *AJ*, 110, 1526
- Jakobsen, P., Bokserberg, A., Deharveng, J. M., Greenfield, P., Jedrzejewski, R., & Paresce, F. 1994, *Nature*, 370, 35
- Jenkins, E. B., & Ostriker, J. P. 1991, *ApJ*, 376, 33
- Kirkman, D., & Tytler, D. 1995, *BAAS*, 27, 848
- Madau, P. 1992, *ApJ*, 389, L1
- Madau, P., & Meiksin, A. 1994, *ApJ*, 433, L53
- Miralda-Escudé, J. 1993, *MNRAS*, 262, 273
- Miralda-Escudé, J., & Ostriker, J. P. 1990, *ApJ*, 350, 1
- Miralda-Escudé, J., Cen, R., Ostriker, J. P. & Rauch, M. 1996, 471, 582
- Møller, P., & Jakobsen, P. 1990, *A&A*, 228, 299
- Nath, B. B. & Sethi, S. K. 1996, *MNRAS*, 279, 275
- Paresce, F., McKee, C., & Bowyer, S. 1980, *ApJ*, 240, 387
- Peterson, B. A. 1978, in *Proceedings of IAU Symposium 79, The Large Scale Structure of the Universe*, ed. M. S. Longair & J. Einasto (Dordrecht: Reidel). 309
- Press, W. H., & Rybicki, G. B. 1993, *ApJ*, 418, 585

- Press, W. H., Rybicki, G. B., & Schneider, D. P. 1993, *ApJ*, 414, 64
- Rauch, M., Carswell, R. F., Webb, J. K., & Weymann, R. J. 1993, *MNRAS*, 260, 589
- Rodríguez-Pascual, P. M., de la Fuente, A., Sanz, J. L., Recondo, M. C., Clavel, J., Santos-Lleó, M., & Wamsteker, W. 1995, *ApJ*, 448, 575
- Sargent, W. L. W., Young, P. J., Boksenberg, A., & Tytler, D. 1980, *ApJS*, 42, 41
- Songaila, A., Hu, E. M., & Cowie, L. L. 1995, *Nature*, 375, 124
- Steidel, C. C., & Sargent, W. L. W. 1987, *ApJ*, 318, L11
- Tytler, D. 1987, *ApJ*, 321, 49
- Zhang, Y., Anninos, P., Norman, M. L. 1995, *ApJ*, 453, L57
- Zheng, W., & Davidsen, A. F. 1995, *ApJ*, 440, L53
- Zheng, W., Kriss, G. A., Telfer, R. C., Grimes, J. P. & Davidsen, A. F. 1997*a*, *ApJ*, 475, 469
- Zheng, W., et al. 1997*b*, in preparation

Fig. 1.— Ratio of He II and H I Ly α decrement vs. column density of neutral hydrogen for a single line. $\xi = b_{He}/b_H = 0.8$ is assumed. Dotted curve: $b_H = 20 \text{ km s}^{-1}$, solid line: $b_H = 30 \text{ km s}^{-1}$, and dashed curve: $b_H = 50 \text{ km s}^{-1}$.

Fig. 2.— Wavelength-averaged He II optical depth produced by the H I forest lines with column density between the minimum value and 10^{17} cm^{-2} . The upper panels hold ξ fixed at 0.8 while varying η , and the lower panels hold η fixed at 100 while varying ξ as shown. The values at the current observation limit, $\log N = 12.3$ are marked, representing the maximum amounts of opacity the observed forest lines can account for. For Figure 2a, the quasar redshift is assumed to be 2.74, and the opacity is calculated for the D_A region, i.e. between 262 and 292 Å in the quasar rest frame. The observed He II opacity, $\tau_{\text{HeII}} = 1.00 \pm 0.07$, in the HUT observation of HS1700+64 is marked by the shaded area. For Figure 2b, the quasar redshift is assumed to be 3.3, and the opacity is calculated between 292 and 303.3 Å in the quasar rest frame, assuming an average H I opacity $\tau_{\text{HI}} = 0.21$, as estimated from the work of Songaila et al. (1995). The shaded region is set by the recent results $\tau_{\text{HeII}} = 2.0_{-0.5}^{+1.0}$ (Hogan et al. 1997).

Fig. 3.— Ratio of ρ He II forest opacity to H I forest opacity vs. minimum column density. A redshift $z_{em} = 2.74$ is assumed, but as discussed in the text, ρ is virtually independent of redshift. The upper panel holds ξ fixed at 0.8 while varying η , and the lower panel holds η fixed at 100 while varying ξ as shown. The values at the current observation limit, $\log N = 12.3$ are marked. The dashed lines represent the expected values derived using Eq. 2 with the same parameters used to generate the curves.

Fig. 4.— Simulated spectrum of quasar Q0302-003. Upper panel: hydrogen forest absorption spectrum, constructed from the fitted lines with column density $N > 10^{12} \text{ cm}^{-2}$ in the Keck spectrum (Hu et al. 1995). Lower panel: He II forest spectrum, constructed by multiplying the optical depth at each pixel by 20 and dividing the wavelengths by 4. The pixel size is 0.04 Å for the H I spectrum and 0.01 Å for He II. The He II spectrum is binned to 2.5 Å for display. It shows an average decrement of 0.60, representing an optical depth of 0.91, which is significantly smaller than that derived by Songaila et al. (1995). Note that the wavelength range used to calculate the $\tau_{\text{HeII}} \approx 2.0$ corresponds to 4960–5120 Å, where the H I opacity is even lower.

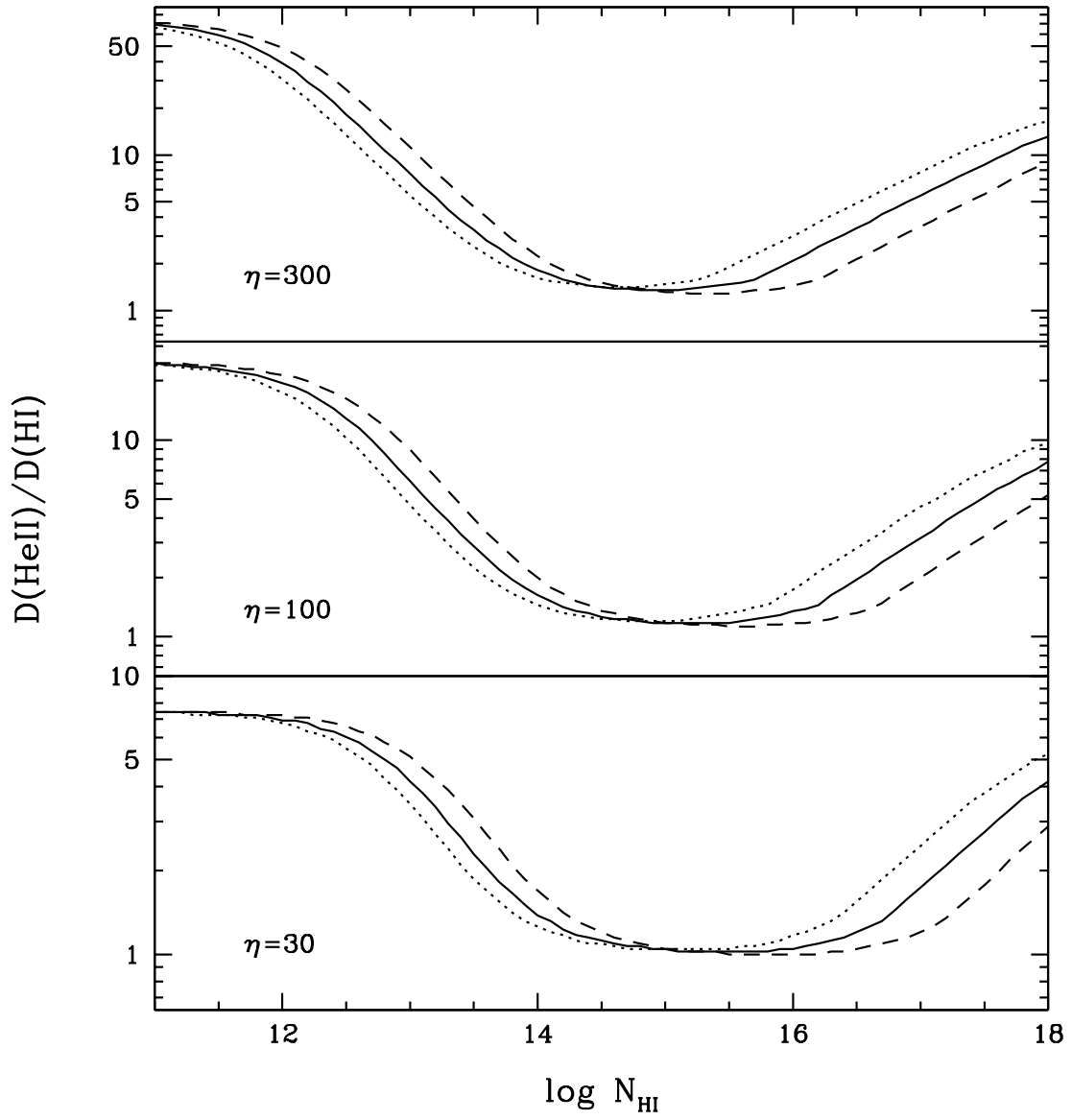


Fig. 1.—

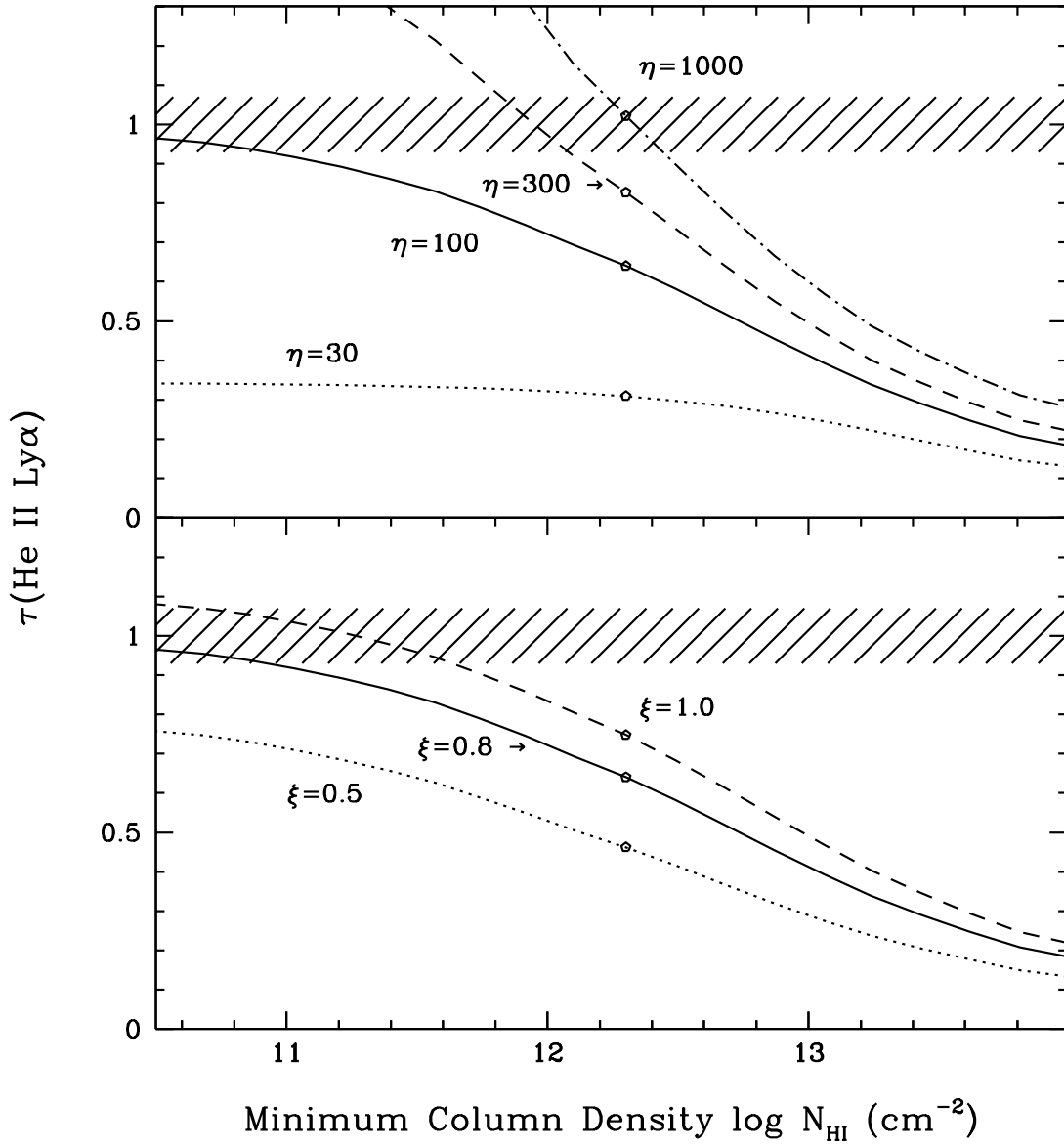


Fig. 2.—

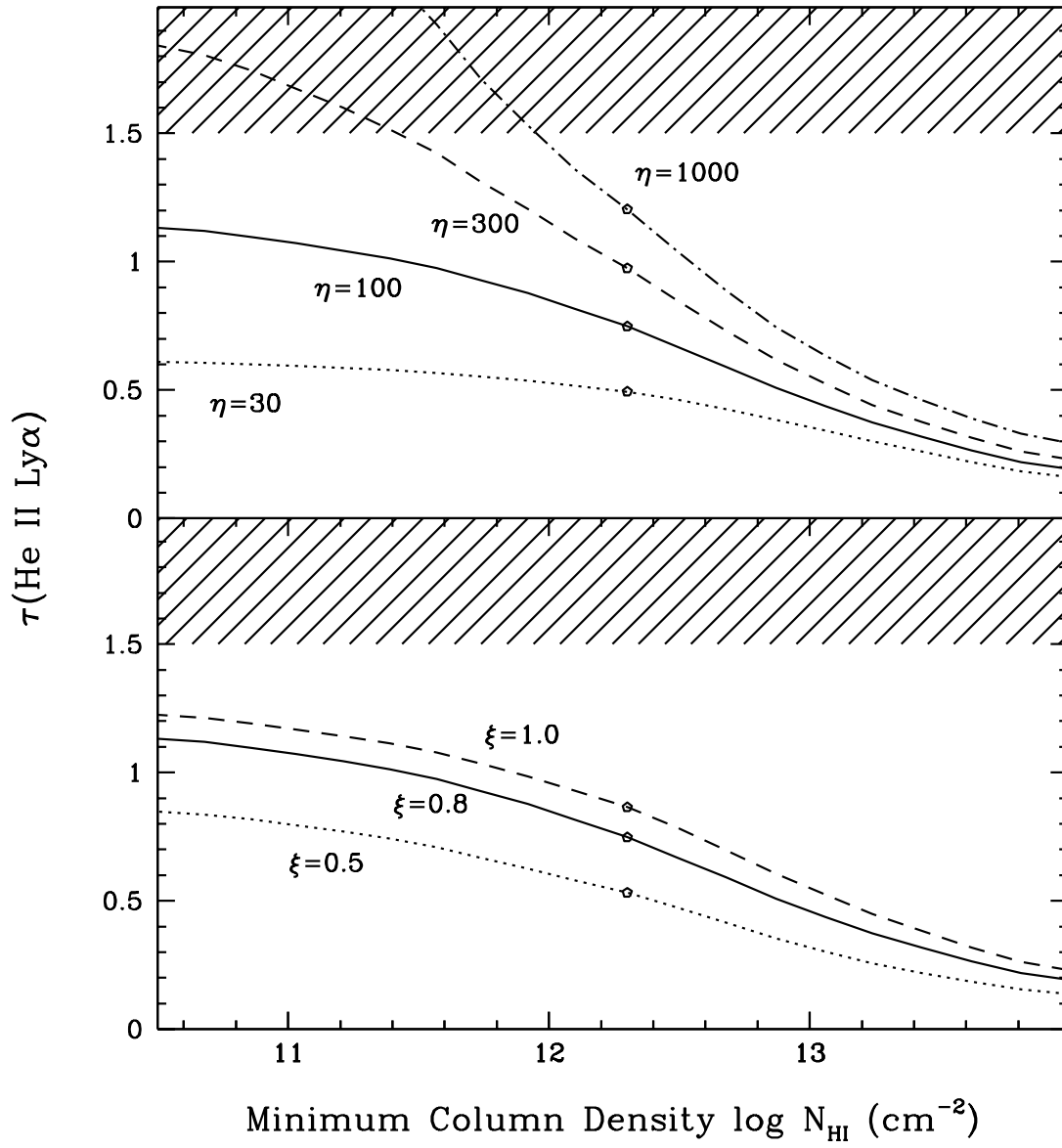


Fig. 2.— continued

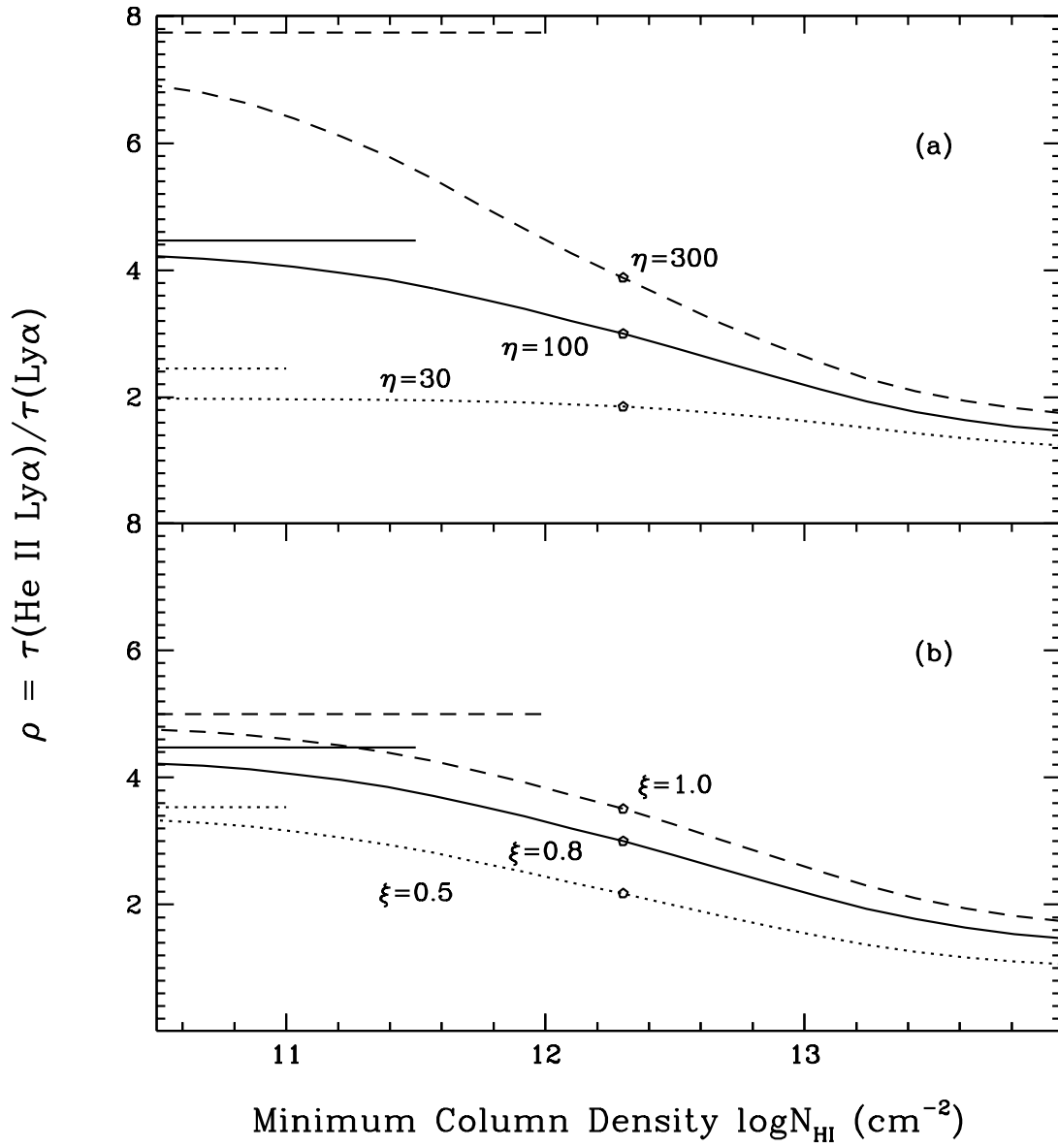


Fig. 3.—

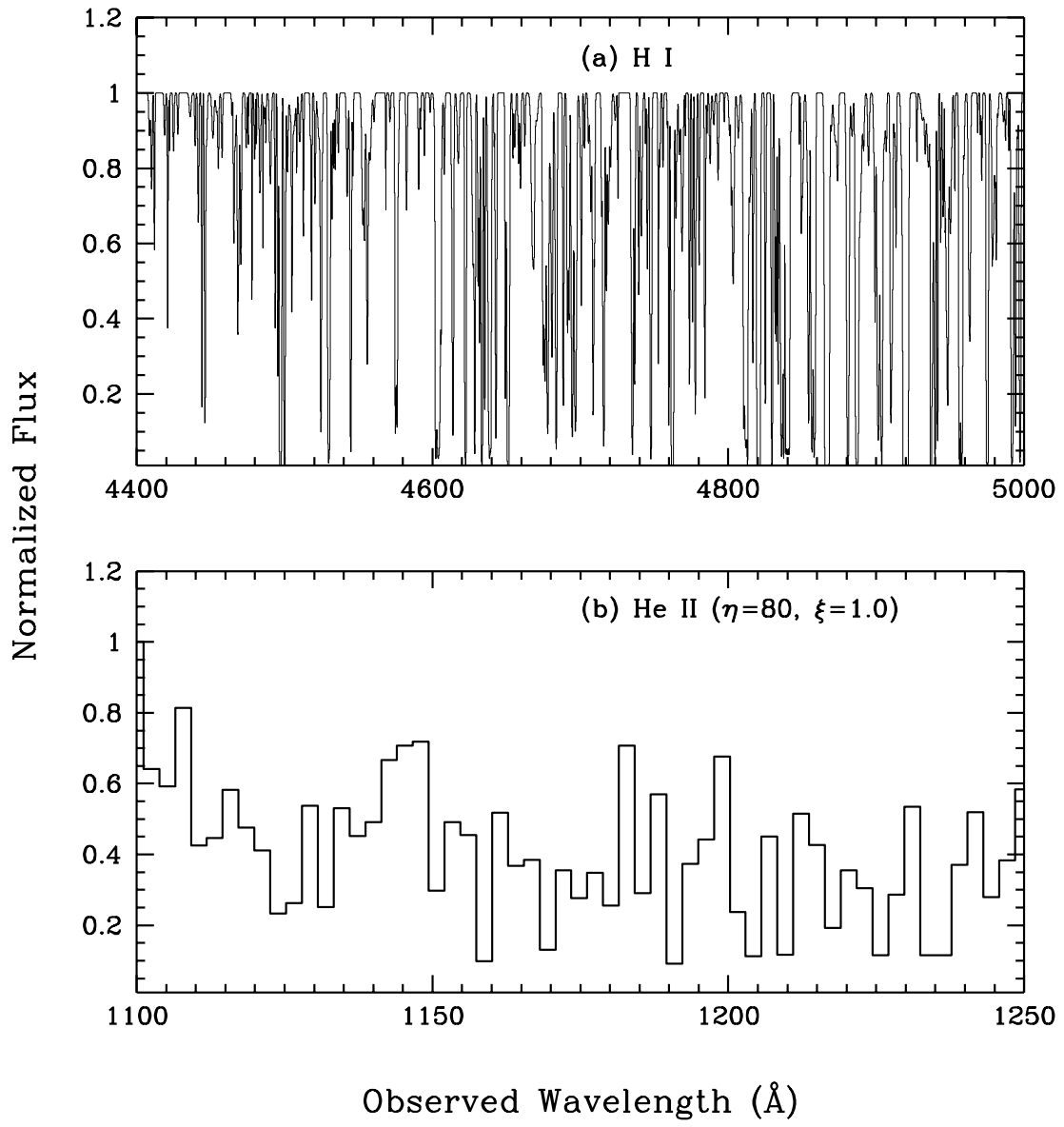


Fig. 4.—